

1 Dear editors and reviewers, thank for your comments and suggestions.

2 Replies for anonymous referee #2 as follows:

3

4 This paper studies InSAR data collected for the 2015 Chile earthquake, in order to determine
5 the fault geometry, the slip distribution and the related distribution of Coulomb stress change,
6 to be compared with the aftershock distribution. The English usage is very poor along all the
7 paper length. I found difficult to follow the description of the work made on INSAR observation,
8 but I am not a specialists of the subject. The motivations of the study, the choice of the inverted
9 data together with their advantages, and the impact of results are not enough discussed. Some
10 specifications are not given for result reproducibility. Some results are not interpreted correctly.

11 **Answer:**

12 (1) We will make a major revision of the manuscript, including redraw Fig.2 expressed as
13 unwrapped displacement instead of phase interferograms, redraw Fig.3 to be clear using good
14 color scale, make another inversion based on curved fault, recalculate Coulomb stress change
15 and redraw Fig.4, add resolution test and strengthen the analysis of the content of the discussion,
16 and so on.

17 (2) We will asked for a native English speakers to modify the finally revised the manuscript
18 text.

19

20 Scientific Significance: 3 Fair. Currently, elastic half space inversions and computation of
21 Coulomb stress changes for planar dislocations requires almost standard techniques.
22 Unfortunately, another paper recently provided a more resolved information about this
23 earthquake, by jointly inverting also other kinds of data and using a more complex geometry of
24 fault (curved surface) and elastic structure (Melgar et al. 2015doi:10.1002/2015GL067369).

25 **Answer:**

26 (1) Melgar et al. really made a very excellent research in this Chile's earthquake (Melgar et al.
27 2015doi:10.1002/2015GL067369), we have read his paper carefully. He used four kinds of data
28 (high-rate GPS records, strong motion records, two interferograms from ascending and
29 descending of the S1A satellite, and tide gauge records) , jointly inverted the fault slip model.
30 They found that this earthquake produced deep and shallow two sliding zones. The “deep”
31 asperity is well separated from the “shallow” asperity by a gap of reduced slip. The deep slip
32 patch extends to 45 km depth, with ~10m peak slip at ~30 km depth. The shallow slip patch
33 ruptured all the way to the trench, with ~10m peak slip at~15 km.

34 (2) Usually, there are some differences in the slip models constrained by different data sets,
35 although it is necessary to use a variety of data sets to get a good slip model. In fact, dense
36 InSAR data can provide good constrain to the near field deformation. In our paper, we used
37 ascending and descending S1A InSAR data to get the coseismic deformation field and invert
38 the slip model. We obtained one slip zone with maximum slip about 8m at ~10km depth, the
39 slip depth reached 45km, while the large slip occurred in shallow portion. These results are
40 similar to that of Melgar's, In addition to his discovery of the two slip areas. Our results are
41 similar to those obtained by Giuseppe Solaro et al.(Giuseppe Solaro et al.
42 2016,doi:10.3390/rs8040323) using S1A data, which indicates our results are correct.

43 (3) In addition, in our manuscript, we calculated and analyzed the Coulomb Failure

44 Stress (CFS) changes and its relation to aftershocks. We also calculate the vertical
45 displacement component and east–west(E-W) displacement component by using the
46 ascending and descending data.

47 (4) We think these results from our study are significant for understanding the fracture
48 behavior of the earthquake. We will improve and perfect this manuscript according to
49 your comments and suggestions in the modified version.

50

51 Scientific Quality: 3 Fair. Results of the Coulomb stress analysis (see below) can be obtained
52 and interpreted more correctly. However, concerning the slip distribution (the extent along dip,
53 the shallow elongation along strike and the relative location with respect to the main-shock
54 hypocentre) the present results are similar to the ones obtained by Melgar et al. (2015). Likely
55 due to the “equal weight” (lines 191-192), results of the joint inversion (ascending plus
56 descending INSAR data) do not differ significantly from those obtained using only descending
57 data. At the same time, model residuals (Figure 2 I-L) are not discussed, so that the joint
58 inversion is not completely justified.

59 **Answer:**

60 (1) We are in favor of your opinion. After reading the comments of the two reviewers,
61 we have realized that a flat fault approximation in our inversion lead to a deviation from
62 the aftershock, at the same time, the results of Coulomb Failure Stress (CFS) changes
63 calculated based on the flat fault model are also affected. We will take new inversion
64 using bending fault plane and recalculate the Coulomb Failure Stress (CFS)
65 changes, and give more correct interpretation in the revised manuscript.

66 (2) We think the reason for the difficulty in distinguishing the results of joint inversion
67 from those obtained using only descending data is due to bad color scale. We will use
68 an appropriate color-scale to distinguish the slip differences of different data sets to
69 make the Fig.3 easy to read in the modified version.

70 (3) The residual in Figure 2 (I - L) is ~15cm, compared with the coseismic displacement more
71 than 130cm, this residual is acceptable. The residual from inversion of ascending or descending
72 data alone is slightly smaller than that from inversion jointly. This may be due to the slip model
73 in joint inversion to meet both ascending and descending data at the same time.

74

75 Presentation Quality: 4 Poor. Besides the poor English usage, the LOS displacement increments
76 shown in figure 2 are scarcely interpretable. Some of the used parameters are not specified.
77 Aftershock hypocenter locations should be evidenced also in cross sections together with the
78 rupture extent (Figure 4c). The same saturating values of Coulomb stress (min/max in the colour
79 palette) should be used both in Figure 4a and 4c. The two tables can be more comprehensively
80 organized.

81 **Answer:**

82 (1) We will invite a native English speaker to modify the final manuscript and adjust
83 some expressions.

84 (2) We will redraw Figure 2 expressed as unwrapped displacement instead of phase
85 interferograms in order to make it easy to explain, and we will redraw Figure 4a, 4c and
86 modify them according to reviewer’s suggestion.

87

88 To be publishable, the paper should improve the presentation and compare its results with that
89 obtained by Melgar et al (2015), with trying to interpret the differences in the light of the
90 different resolving power of the data used and the different modelling assumption made.

91 **Answer:**

92 As mentioned above, we will take new inversion using bending fault plane and
93 recalculate the Coulomb Failure Stress (CFS) changes, strengthen the content of the
94 discussion section through the comparison with that of Melgar et al (2015).

95

96 **Detailed comments:**

97

98 Line 70, 212 and 218 “shear” -> “Coulomb”

99 **Answer:**

100 It has been modified in the revised manuscript.

101

102 Line 142: “Firstly”: Before making the linear inversion for the slip distribution, authors make
103 the nonlinear joint inversion (of both ascending and descending data) for the fault geometry
104 (optimal model, results shown in Table 2). Unlike the inversion for the slip distribution, in the
105 nonlinear inversion authors do not consider separately ascending and descending InSAR data.

106 **Answer:**

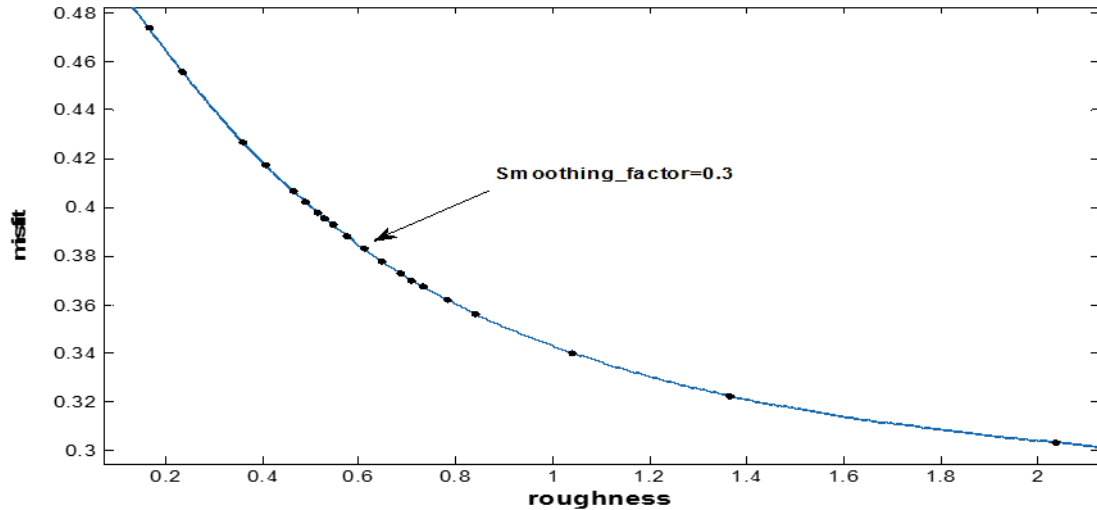
107 Our fault slip inversion following two steps: firstly, we carry out a nonlinear inversion
108 to constrain the fault geometry, then we perform a linear inversion to retrieve the fault
109 distribution. Different data sources can get different fault geometry in the nonlinear
110 inversion. When we make a nonlinear inversion constrained by ascending data, the
111 obtained fault model has poor fitting to descending data, and vice versa. In order to get
112 a general fault geometry, we use both ascending and descending data in the nonlinear
113 joint inversion.

114

115 Line 151-152 I agree with referee 1: the criterion used to choose the smoothing factor (beta)
116 and its chosen value should be declared.

117 **Answer:**

118 We select the smoothing factor through trade-off curve model between roughness and
119 misfit which are mutually restricted. When the smooth factor value increase, the misfit
120 value will increase, while the roughness will decrease. By using a trade-off curve
121 (Figure S1.), we find best fitting smoothing factor 0.3 for descending data inversion.
122 Taking into account the degree of constraint by smooth factor in fault slip inversion is
123 similar, the smoothing factor is all set to 0.3 in our three kinds of inversion.



124

125 **Figure S1.** The trade-off curve between roughness and misfit

126

127 Line 160 “is to the surface” -> “is put at the surface of the elastic half-space”.

128 **Answer:**

129 It has been modified in revised manuscript.

130

131 Table 2 misses the average value of slip and rake assumed or estimated. Parameters fixed or
 132 estimated should be distinguishable in Table 2. In Table 2, rather than in Table 3, I would
 133 suggest the authors to compare the results of the optimal model with evidences from USGS and
 134 GCMT.

135 **Answer:**

136 We will add the corresponding contents to table 2 and table3 according to your opinion
 137 in our revised manuscript.

138

139 Table 3: it is necessary to declare the shear modulus (or rigidity) value used to estimate the
 140 seismic moment, as reported in the last three rows. On the contrary, here reporting the same
 141 data concerning dip and strike as in Table 2 is unnecessary. Reporting the maximum slip
 142 together with the depth of the down-dip edge of the rupture, according to the different data sets,
 143 should help readers in understanding how the inferred results depend on the particular data set.
 144 Please check the rake angle estimated with descending data which is declared as 110_ at line
 145 177.

146 **Answer:**

147 We set the shear modulus 3.0×10^6 MPa in our fault slip inversion. We will modify table
 148 2 and table 3 to add the corresponding contents mentioned above in the revised
 149 manuscript

150

151 Lines 178, 185 and 194. I am surprised that the “fitting degree” (not defined) is so high, giving
 152 the results shown in Figure 2 I-L.

153 **Answer:**

154 (1) The fitting degree is defined as follows:

155

$$Corr = \frac{\sum_{n=1}^N O_n \cdot P_n}{\sqrt{\sum_{n=1}^N O_n^2 \cdot \sum_{n=1}^N P_n^2}}$$

156

'Corr' is the fitting degree, 'n' is the data points index, 'N' is the total sampled points in our inversion. 'O' is the observation data. 'P' is the prediction data. When $O_n \approx P_n$, $Corr \approx 1$.

157

158

159

(2) The residual error of the observed value minus the model is about 15cm (Figure2 I-L), compared with the coseismic displacement more than 130cm, this residual is small and acceptable, so the "fitting degree" is high.

160

161

162

(3) We will redraw the Fig.2 to make the residual value easy to identify.

163

164

Line 181. What is the "scope" of the slip magnitude? Concerning the lower slip values or seismic moment estimated with ascending data, referee 1 gives an interpretation more articulated and convincing, than the one given by the authors. The displacement observed at a GPS station is a useful constraint to solve for the true displacement observed in the LOS direction.

165

166

167

168

169 **Answer:**

170

(1) Here the "scope" of the slip magnitude means the range of the slip area coverage on fault plane. We will improve the English expression in revised version.

171

172

(2) We agree with you. We are aware of the two question after reading the review comments. On the one hand, the much smaller slip value in ascending data inversion is likely to be related to the unwrapping, on the other hand, the color scale we used is not appropriate, so that distinction is not clear. We will seriously examine and revise these issues in order to improve the clarity and quality of the map in the revised manuscript.

173

174

175

176

177

(3) As you said, it is very good to use the displacement observed at a GPS station as constraint to solve for the true displacement observed in the LOS direction. In the observation of coseismic deformation, We usually take the far field without deformation fringes as reference when the GPS is not available in the region of interferogram. That's what we did in this manuscript. We will check and improve the process of unwrapping in the new version.

178

179

180

181

182

183

184

Line 211. Stain->Stein. I agree with referee 1: likely aftershocks appear below the fault, because the true fault curvature is neglected. Often, the distribution of the seismicity hypocentres, possibly relocated, in a vertical cross section, allows us to delineate the true dip of the mainshock fault.

185

186

187

188 **Answer:**

189

(1) "Stain" has been modified to "Stein" in the revised manuscript.

190

191

(2) We agree with the comments of the reviewers. We have realized that a flat fault approximation in our inversion does lead to a deviation from the aftershocks. The dip angle of the seismogenic fault may be greater in the deeper part. So we will take new inversion using bending fault plane in the revised manuscript, which will improve our interpretation.

192

193

194

195

196 Line 214. In general, the distribution of aftershock is not used to choose the “receiver fault
197 mechanism”. If the concern are aftershocks, the best thing to do is considering their focal
198 mechanism in order to determine the” mechanism of the receiver fault”. As said, aftershock
199 alignments suggest the geometry of the “source fault” (where the mainshock occurred),
200 therefore choosing this geometry for the “receiver fault” coincides with assuming that
201 aftershocks occurred on faults with the same fault mechanism as the source fault. We cannot
202 state that the authors chose this last strategy because in this paper the source fault does not have
203 the same dip as inferred from aftershock alignments.

204 **Answer:**

205 After reading the comments of two reviewers, we have noticed this deviation caused by
206 the flat plane fault approximation in our inversion. The aftershock distribution should
207 reflect the geometry of the main fault. That is to say the dip angle of the seismic fault
208 becomes larger in the deeper portion (about 20 km below). The flat fault model leads
209 to inappropriate interpretation. In the revised manuscript, we will take new inversion
210 using bending fault plane and compare with the old one, and give more reasonable
211 interpretation.

212

213 Line 218-222: The following two statements are scarcely supported by Figure 4 results:

214 1) “(we) find aftershocks (depth in 20km-30km) locations correlate well with the area shaving
215 increased Coulomb stress”, 2) “most areas with increased Coulomb stress appeared beneath the
216 main shock fault plane, which is consistent with the location where aftershocks took place.”

217 **Answer:**

218 We agree with you. The statements in our initial manuscript are really inappropriate due
219 to the deviation from the plane fault approximation. We will make a new inversion
220 using bending fault and recalculate the Coulomb Failure Stress (CFS) changes, redraw
221 the Fig.4, we will add aftershocks to Fig.4C to make the relationship between the CFS
222 changes and the aftershock distribution more clear and easy to judge in our revised
223 manuscript.

224

225 1) Actually in Figure 4a the majority of aftershocks seems to be shadowed (negative coulomb
226 stress change) by the main rupture. This suggest that the 30 km of depth of the map view is
227 above the down-dip edge of the rupture at least close to line B-B’ (as also stated at lines 19,
228 278, 295). If this is true, the positive Coulomb stress values within the horizontal projection of
229 the fault rupture likely are not due to the slip distribution, given the absence of asperities
230 (regions of no slip) within the rupture surface, as evident from Figure 3c. In obtaining this result,
231 a role may have the change in the receiver dip with respect to the source dip (see last point), or
232 numerical problems due to fault discretization near the fault plane, evident mainly in cross
233 sections (Figure 4c).

234 **Answer:**

235 Under the guidance of the referee's opinions, We do realize that the results shown in
236 Fig.4 and corresponding explanation are not appropriate. Maybe the flat fault model
237 with low dip angle(18.3°) used in our initial manuscript leads to the deviation of the
238 source fault from the distribution of the aftershock, and the inappropriate location

239 settings of the receiver fault. These issues will be all modified in the revised manuscript
240 by making new inversion based on curved fault and recalculating CFS.

241

242 2) In Figure 4c, below the fault plane, the most reliable positive feature is the off-fault lobe of
243 Coulomb stress, which is located at a distance of about 200 km. It is due to tensile stress changes
244 caused by the main rupture (the so-called antithetic lobe). However few of the aftershocks
245 reported in Figure 4b seem to locate there.

246 **Answer:**

247 The off-fault lobe of Coulomb stress with positive value appears in the deep near the
248 trench (Figure 4c), We think there may be several factors that can lead to this
249 phenomenon: for example, aseismic slip and low initial stress accumulation in the area.
250 In our revised manuscript, we will give a more reasonable explanation based on new
251 CFS calculation results and relevant referencs.

252

253 Lines 273-275 Sentence to be rewritten for clarity.

254 **Answer:**

255 We will carefully revise these sentences in the revised manuscript.

256